THE JOURNAL OF BIOLOGICAL CHEMISTRY
Vol. 280, No. 16, Issue of April 22, pp. 16368–16376, 2005
Printed in U.S.A.

Compensatory Contributions of HEXIM1 and HEXIM2 in Maintaining the Balance of Active and Inactive Positive Transcription Elongation Factor b Complexes for Control of Transcription*

Received for publication, January 25, 2005
Published, JBC Papers in Press, February 14, 2005, DOI 10.1074/jbc.M500912200

Jasper H. N. Yik‡, Ruichuan Chen‡§, Andrea C. Pezda‡, and Qiang Zhou‡¶

From the ‡Department of Molecular and Cell Biology, University of California, Berkeley, California 94720 and §School of Life Sciences, Xiamen University, Xiamen 361005, China

Human positive transcriptional elongation factor b (P-TEFb), consisting of a cyclin-dependent kinase 9-cyclin T heterodimer, stimulates general and disease-specific transcriptional elongation by phosphorylating RNA polymerase II. The HEXIM1 protein, aided by the 7SK snRNA, sequesters P-TEFb into an inactive 7SK·HEXIM1·P-TEFb small nuclear ribonucleic acid particle for inhibition of transcription and, consequently, cell proliferation. Here we show that, like HEXIM1, a highly homologous protein named HEXIM2 also possesses the ability to inactivate P-TEFb to suppress transcription through a 7SK-mediated interaction with P-TEFb. Furthermore, HEXIM1 and HEXIM2 can form stable homo- and hetero-oligomers (most likely dimers), which may nucleate the formation of the 7SK small nuclear ribonucleic acid particle. Despite their similar functions, HEXIM1 and HEXIM2 exhibit distinct expression patterns in various human tissues and established cell lines. In HEXIM1-knocked down cells, HEXIM2 can functionally and quantitatively compensate for the loss of HEXIM1 to maintain a constant level of the 7SK/HEXIM-bound P-TEFb. Our results demonstrate that there is a tightly regulated cellular process to maintain the balance between active and inactive P-TEFb complexes, which controls global transcription as well as cell growth and differentiation.

RNA polymerase II mediates transcription of all class II protein-coding genes in a tightly regulated process that can be divided into five stages: preinitiation, initiation, promoter clearance, elongation, and termination (1). It is during the elongation phase that the positive transcriptional elongation factor b (P-TEFb)[1] phosphorylates the carboxyl-terminal domain of the largest subunit of RNA polymerase II. This event is crucial for the transition from the abortive to the productive phase of transcriptional elongation, leading to the generation of full-length RNA transcripts (for reviews, see Refs. 2 and 3). Not only is P-TEFb essential for the expression of most protein-encoding genes (4, 5), it is also indispensable for the replication of HIV-1. P-TEFb is a specific host cellular cofactor for the viral Tat protein, which recruits P-TEFb to the HIV-1 promoter to greatly enhance viral gene transcription (2, 3).

The core P-TEFb, composed of CDK9 and its regulatory cyclin subunit T1, T2, or K (3), exists in two major forms in the cell. The kinase inactive form contains core P-TEFb in association with its inhibitors 7SK snRNA and HEXIM1 in a single 7SK snRNP, whereas the active form is 7SK/HEXIM1-free (6–9). Although P-TEFb is the primary binding partner and target of HEXIM1, the association of P-TEFb with HEXIM1 itself is very weak. This interaction is greatly enhanced in the presence of the non-coding 7SK snRNA (7, 9, 10), which interacts with both P-TEFb and HEXIM1 through the central arginine-rich 7SK-binding/nuclear localization signal (NLS) domain and acts as a scaffold for the assembly of P-TEFb with HEXIM1 (11). Once associated with HEXIM1, P-TEFb loses it kinase activity and is unable to phosphorylate the RNA polymerase II carboxyl-terminal domain and stimulate transcriptional elongation (7, 9, 11).

The association of 7SK/HEXIM1 with P-TEFb is a dynamic process and can be disrupted by certain stress-inducing agents, such as the global transcriptional inhibitor actinomycin D, kinase/transcription inhibitor 5,6-dichloro-1-β-D-ribofuranosylbenzimidazole (DRB), DNA-damaging agent UV irradiation, as well as cardiac hypertrophic signals (6–12). A shift in the balance between active P-TEFb and the inactive, 7SK/HEXIM1-bound P-TEFb can have serious physiological consequences. For example, disruption of the 7SK ribonucleic acid particle by hypertrophic signals has been shown to activate P-TEFb in cardiac myocytes, leading to an increase in phosphorylation of RNA polymerase II that results in a global elevation of RNA and protein contents (12). This chain of events eventually causes the enlargement of heart cells that leads to cardiac hypertrophy. This observation has been confirmed independently by ablation of the mouse HEXIM1 (CLP-1) gene, which leads to cardiac hypertrophy and embryonic lethality (13).

HEXIM1 has previously been identified as a nuclear protein whose expression is rapidly induced in human smooth muscle cells as well as in many other cell types that are treated with hexamethylene bisacetamide (HMBA) (14),[2] a potent inducer of

* This work was supported by National Institutes of Health Grant AI41757 and American Cancer Society Grant RSG-01-171-01-MBC (both to Q. Z.), Ruth L. Kirschstein NRSA Individual Post-doctoral Fellowship AI058400 from the National Institutes of Health (to J. H. N. Y.), and a Berkeley Scholar Fellowship (to R. C.). The costs of publication of this article were defrayed in part by the payment of page charges. This article must therefore be hereby marked "*advertisement*" in accordance with 18 U.S.C. Section 1734 solely to indicate this fact.

¶ To whom correspondence should be addressed: Dept. of Molecular and Cell Biology, University of California, Berkeley, 622 Barker Hall, #3202, Berkeley, CA 94720-3202. E-mail: qzhou@uclink4.berkeley.edu.

[1] The abbreviations used are: P-TEFb, positive transcription elongation factor b; CDK, cyclin-dependent kinase; CycT1, cyclin T1; DRB, 5,6-dichloro-1-β-D-ribofuranosylbenzimidazole; HMBA, hexamethylene bisacetamide; NE, nuclear extract; NLS, nuclear localization signal; snRNP, small nuclear ribonucleic acid particle; GST, glutathione *S*-transferase; HIV, human immunodeficiency virus; HA, hemagglutinin.

[2] J. H. N. Yik, R. Chen, A. C. Pezda, and Q. Zhou, unpublished observations.

cell differentiation and suppressor of cell proliferation (15). On the other hand, HEXIM1 has also been identified as an inhibitor of breast cell proliferation, and HEXIM1 expression is down-regulated by estrogens and decreased in breast tumors (16). The observed anti-growth function of HEXIM1 in many cell types suggests that regulation of the activity of P-TEFb through changes in HEXIM1 expression or its P-TEFb-targeting capability could potentially play a key role in directing the cells toward either proliferation or differentiation.

Sequence analysis has indicated that a hypothetical protein (GenBank™ accession number AK056946), hereby renamed as HEXIM2, showed a high degree of homology with HEXIM1 (10). However, the expression of the HEXIM2 protein has not been confirmed, and whether it possesses a function similar to that of HEXIM1 has yet to be established. In this study, we examined the expression patterns of HEXIM1 and HEXIM2 in various human tissues and compared the inhibitory effects of HEXIM1 and HEXIM2 on P-TEFb activity in order to gain insights into the physiological function of HEXIM2.

EXPERIMENTAL PROCEDURES

Materials—HeLa and 293T cells were purchased from American Type Culture Collection (Manassas, VA). U373, SK-Hep-1, IMR-90, TK6, and CaCo-2 cells were a generous gift from the University of California, Berkeley tissue culture facility. Rabbit anti-CDK4, -CDK9, and -CycT1 antibodies were purchased from Santa Cruz Biotechnology (Santa Cruz, CA). FLAG peptide, mouse anti-FLAG antibody, and anti-FLAG or anti-HA antibody conjugated to agarose beads were obtained from Sigma. Mouse anti-tubulin antibody was from Oncogene. The generation of rabbit anti-HEXIM1 antibody was described previously (7). Rabbit anti-HEXIM2 antibody was generated against its amino-terminal sequence TSGAPGSPQTPPERHDSG. Rabbit anti-HEXIM antibody that recognizes both HEXIM1 and HEXIM2 was generated against a highly conserved peptide DFSETYERFHTESLQ shared by the two proteins, except that HEXIM1 has a single Phe to Tyr substitution at position 9 (see Fig. 1*A*). Buffer D contained 20 mM HEPES-KOH, pH 7.9, 15% glycerol, 0.2 mM EDTA, 0.2% Nonidet P-40, 1 mM dithiothreitol, 1 mM phenylmethylsulfonyl fluoride, and various concentrations of KCl as indicated below. RNase A was obtained from Roche Applied Science. All other chemicals were from Sigma unless otherwise noted.

To generate the H2C5 cell line stably expressing FLAG-HEXIM2, HeLa cells were transduced with the pBabe-puro-based retrovirus (17) that expressed FLAG-tagged HEXIM2. The puromycin-resistant cell line H2C5 was selected and propagated as described previously (6).

Plasmid Constructs—FLAG-tagged HEXIM2 expression construct was generated by insertion of the PCR fragment amplified from HEXIM2 cDNA (clone 4559410; Invitrogen) into the pFLAG-CMV2 vector (Sigma) at the EcoRI and SalI sites. FLAG-tagged HEXIM1 in pFLAG-CMV2 was a generous gift from Dr. H. Tanaka (University of Tokyo). HA-tagged HEXIM1 and HEXIM2 constructs were generated by PCR fusion of the HA sequence amino-terminally to the HEXIM1 and HEXIM2 open reading frames and cloned into the pcDNA3 vector (Invitrogen).

Affinity Purification of HEXIM Proteins and Their Associated Factors—For Western and Northern analyses, FLAG- or HA-tagged HEXIM proteins were expressed from cDNA constructs in HeLa cells transfected with the Lipofectamine Plus reagent (Invitrogen). Nuclear extract (NE) was prepared from the transfected cells 48 h later, as described previously (18). The HEXIM complexes were affinity-purified from the extracts by incubation at 4 °C for 2 h with anti-FLAG- or anti-HA-agarose beads, followed by extensive washes with Buffer D containing 0.3 M KCl and elution with the FLAG or HA peptide dissolved in Buffer D containing 0.1 M KCl. The eluted materials were analyzed by Western blotting with anti-FLAG, anti-CDK9, anti-CycT1, and anti-HEXIM antibodies and Northern hybridization using the full-length 7SK antisense RNA as a probe as described previously (6). For *in vitro* kinase and transcription assays, individually transfected FLAG-tagged HEXIM1 and HEXIM2 proteins were affinity-purified by anti-FLAG-agarose beads from NE of transiently transfected 293T cells. After extensive washes with Buffer D containing 1.0 M KCl (to remove the associated 7SK and core P-TEFb) followed by washes with Buffer D containing 0.05 M KCl, the immobilized FLAG-HEXIM proteins were eluted with 0.5 mM FLAG peptide in Buffer D containing 0.05 M KCl and 1 mg/ml bovine serum albumin.

In Vitro Kinase and Transcription Assays—*In vitro* kinase reactions were performed essentially as described previously (7). *In vitro* transcription reactions containing normal or CDK9-depleted HeLa NE (dialyzed in Buffer D containing 0.1 M KCl) and a pair of HIV-1 transcription templates were performed essentially as described previously (19), with slight modifications. NE was first pre-incubated at 30 °C for 20 min with the affinity-purified FLAG-HEXIM proteins in the presence of 0.5 mM ATP and 5 mM $MgCl_2$. This step facilitated the phosphorylation of the endogenous 7SK/HEXIM-free P-TEFb in NE and thus facilitated the subsequent binding of the exogenously added HEXIM proteins to 7SK/P-TEFb (20). The core P-TEFb was generated by immunoprecipitation from F1C2 NE containing CDK9-FLAG, treatment with RNase A and high salt to remove HEXIM/7SK from P-TEFb, and then elution with the FLAG peptide. The HEXIM2/7SK-bound P-TEFb was affinity-purified from H2C5 NE harboring FLAG-HEXIM2.

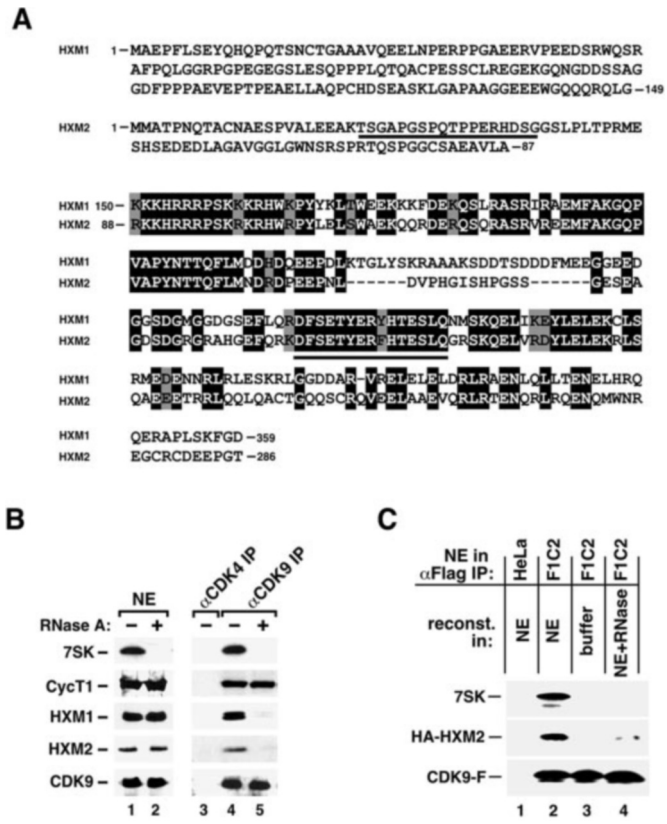

FIG. 1. **HEXIM2 is an integral component of endogenous 7SK snRNP.** *A*, sequence alignment of the human HEXIM1 and HEXIM2 proteins. *Black boxes* indicate amino acid identity, and *gray boxes* indicate similarity. *Underlined peptide sequences* were selected for generation of rabbit polyclonal antibodies. *B*, HEXIM2 is present in the endogenous 7SK·P-TEFb snRNP. HeLa NE was first treated with RNase A (*lane 2*) or left untreated (*lane 1*) and then subjected to immunoprecipitation with either anti-CDK9 (*lanes 4* and *5*) or, as a negative control, anti-CDK4 antibodies (*lane 3*). The immunoprecipitates were analyzed by Western and Northern blotting to detect the individual components. *C*, *in vitro* binding of HEXIM2 to P-TEFb is 7SK-dependent. Anti-FLAG beads were incubated with NE derived from HeLa cells or the HeLa-based F1C2 cells stably expressing FLAG-CDK9, followed by extensive washes with a high salt buffer (Buffer D containing 1.0 M KCl) to remove the associated 7SK snRNA and HEXIM proteins. The immobilized core P-TEFb was than incubated with either buffer only (*lane 3*) or HeLa NE containing HA-tagged HEXIM2 (*lanes 1*, *2*, and *4*), in the presence (*lane 4*) or absence (*lane 2*) of RNase A, to reconstitute the binding of HEXIM2 to P-TEFb. The indicated proteins and 7SK RNA retained on the beads were analyzed by Western and Northern blotting.

Luciferase Assay—HeLa cells (70–80% confluence) grown in 6-well plates were co-transfected with 100 ng of a luciferase reporter construct driven by the HIV-1 long terminal repeat and with increasing concentrations of plasmids expressing either FLAG-tagged HEXIM1 or HEXIM2. The total amount of plasmids (1.3 μg) was kept constant for each transfection by adjusting with the empty vector. Luciferase activity was measured 48 h later with a luciferase assay kit from Promega.

Treatment of Cells with Stress-inducing Agents—H2C5 cells (3×10^6) were seeded in 15-cm dishes 1 day before the treatment with actino-

mycin D (100 μM) and DRB (1 μg/ml). NE was prepared from the treated cells 1 h later.

Northern Tissue Blots—The mRNA levels of HEXIM1 and HEXIM2 in various human tissues were determined by Northern analysis using a FirstChoice™ Human Blot 2 (Ambion). Full-length cDNA fragments of HEXIM1 and HEXIM2 were amplified by PCR and subsequently used with the Stip-EZ™ DNA Kit (Ambion) to generate random-primed ^{32}P-radiolabeled DNA probes. The Northern blot was hybridized overnight and then washed according to the manufacturer's instructions.

Glycerol Gradient Analysis—HeLa cells were co-transfected in a 1:10 ratio with the pBabe-puro empty vector and the pSuper-based vector harboring siRNA562 that target HEXIM1 (7). After 24 h, untransfected cells were killed by the addition of 1.5 μg/ml puromycin into the culturing media. NE was prepared 48 h later and subjected to ultracentrifugation in a Sorvall SW41 rotor at 38,000 rpm and 4 °C for 21 h, in a 10-ml glycerol gradient solution (10–30%) containing 20 mM HEPES, pH 7.9, 0.3 M KCl, 0.2 mM EDTA, and 0.1% Nonidet P-40. Ten fractions were collected, and the proteins in each fraction were precipitated by 70% trichloroacetic acid and analyzed by Western blot as described above.

RESULTS

HEXIM1 and HEXIM2 Share Extensive Sequence Homology at Their Central 7SK-binding/NLS and Carboxyl-terminal Domains—Given the important physiological role of HEXIM1 in controlling transcriptional elongation, it is essential to determine whether other HEXIM1-related protein(s) may possess functions that are either complementary to or distinct from that of HEXIM1. Homology search of existing cDNA data bases using the 359-amino acid human HEXIM1 sequence revealed that only one predicted human protein of 286 amino acids (GenBank™ accession number AK056946), now renamed HEXIM2, shared extensive homology with HEXIM1. Sequence alignment between HEXIM1 and HEXIM2 showed that the area of homology (>50% identical) begins at the amino-terminal boundary of the central arginine-rich 7SK-binding/NLS domain (amino acids 150–177 of HEXIM1) (11) and extends into the carboxyl-terminal domain of HEXIM1 until position 343 (Fig. 1*A*). In contrast, sequences in their amino-terminal regions are mostly unrelated. The unique amino-terminal half of HEXIM1 has been shown to play a regulatory role because the deletion of this region results in a mutant HEXIM1 that targets and inactivates P-TEFb with higher efficiency than the wild-type protein (7). These observations suggest that whereas the two homologous HEXIM proteins are likely to have similar physiological functions and/or mechanisms of action, they may be regulated differently through their regions of unique sequences.

HEXIM2 Is a Novel Component of the Endogenous 7SK snRNP—To determine whether HEXIM2, like HEXIM1, is also an integral component of the 7SK·P-TEFb snRNP, endogenous CDK9 and its associated factors were affinity-purified from HeLa NE by anti-CDK9 immunoprecipitation and analyzed by Western and Northern blotting. As expected, 7SK, CDK9, CycT1, and HEXIM1 were detected in the anti-CDK9 immunoprecipitates (Fig. 1*B*, *lane 4*), but not in the control precipitates using anti-CDK4 antibody (*lane 3*). In addition, using an antibody generated against a unique amino-terminal peptide derived from HEXIM2 (Fig. 1*A*), a protein matching the predicted ~50-kDa size of HEXIM2 was also detected (Fig. 1*B*, *lane 2*). This same band also reacted to a second antibody that was raised against a highly conserved peptide (Fig. 1*A*; also see "Experimental Procedures") shared by both HEXIM1 and HEXIM2 (see Fig. 6*C*), confirming its identity as HEXIM2. Similar to the 7SK-dependent association of HEXIM1 with P-TEFb (7, 10), the HEXIM2-P-TEFb interaction was also 7SK-dependent, as indicated by the disappearance of HEXIM2 in the CDK9 immunoprecipitates upon the destruction of 7SK with RNase A (Fig. 1*B*, *lane 5*).

Next, an *in vitro* reconstitution system (7) was used to test the ability of HEXIM2 to associate with immobilized P-TEFb in the presence or absence of RNase A. When NE derived from HeLa cells transfected with the HA-tagged HEXIM2 was incubated with immobilized P-TEFb (immunoprecipitated from NE of F1C2 cells stably expressing CDK9-FLAG) (6), HEXIM2 was specifically retained on the P-TEFb beads only when 7SK remained intact in the extract (Fig. 1*C*, compare *lanes 2* and *4*). These *in vivo* and *in vitro* results, together with another one described in Fig. 5*A*, which employed DNA oligonucleotide-directed RNase H cleavage to specifically target 7SK, confirmed the 7SK-dependent nature of the HEXIM2-P-TEFb interaction.

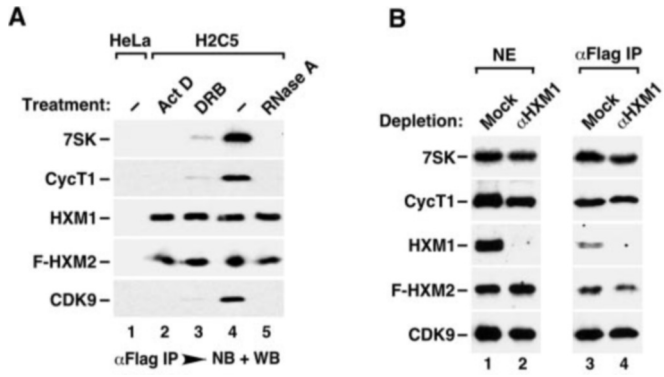

FIG. 2. **Direct interactions of HEXIM2 with HEXIM1 and 7SK/P-TEFb.** *A*, stable HEXIM1-HEXIM2 interaction is unaffected by the removal of 7SK and P-TEFb. The HeLa-based H2C5 cells stably expressing FLAG-tagged HEXIM2 were treated with actinomycin D or DRB. NE from drug-treated and untreated cells was than subjected to immunoprecipitation with anti-FLAG beads in the presence or absence of RNase A. The immunoprecipitates were analyzed by Western and Northern blotting. *B*, HEXIM2 can directly interact with 7SK/P-TEFb in the absence of HEXIM1. HeLa NE containing transiently transfected FLAG-tagged HEXIM2 was first subjected to mock or anti-HEXIM1 immunodepletion, and the HEXIM2-associated factors were then isolated with anti-FLAG beads. The depleted NE and the anti-FLAG immunoprecipitates were analyzed by Western and Northern blotting as indicated.

Stable and 7SK/P-TEFb-independent Interaction of HEXIM2 with HEXIM1—To further characterize the interaction of HEXIM2 with the 7SK·P-TEFb snRNP, a HeLa-based cell line (H2C5) stably expressing the FLAG-tagged HEXIM2 (F-HXM2) was generated and then treated with two stress-inducing agents, actinomycin D and DRB, which are known to cause the disruption of the 7SK·HEXIM1·P-TEFb snRNP (6–10). F-HXM2 and its associated factors were immunoprecipitated from NE of treated cells and analyzed by Western and Northern blotting. In addition to the expected CDK9, CycT1, and 7SK, HEXIM1 was surprisingly found to also associate with HEXIM2 (Fig. 2*A*, *lane 4*). As in the case involving HEXIM1, 7SK and P-TEFb could be dissociated from HEXIM2 in actinomycin D- and DRB-treated cells (Fig. 2*A*, *lanes 2* and *3*). However, the interaction between HEXIM1 and HEXIM2 was not affected by the drug treatments, which dissociated 7SK and P-TEFb (*lanes 2* and *3*), nor was it affected by the degradation of 7SK with RNase A (*lane 5*). Thus, HEXIM1 and HEXIM2 formed a stable complex, whose integrity was not affected by the removal of 7SK and P-TEFb. However, it was not clear from this experiment whether such a complex existed in or outside the 7SK·P-TEFb snRNP.

HEXIM2 Can Directly Interact with 7SK/P-TEFb in the Absence of HEXIM1—In light of the above-described HEXIM1-HEXIM2 interaction and the ability of HEXIM2 to co-immunoprecipitate with 7SK and core P-TEFb, we asked whether HEXIM2 bound directly to 7SK/P-TEFb or indirectly via HEXIM1, which had been shown to associate with 7SK/P-TEFb directly (7, 9–11, 20). To address this question, NE from HeLa cells transiently expressing F-HXM2 was first immunodepleted

of endogenous HEXIM1 (Fig. 2*B*, *lane 2*) and then subjected to anti-FLAG immunoprecipitation to isolate the F-HXM2-associated factors. Western and Northern analyses revealed that 7SK and P-TEFb were able to associate with HEXIM2 in both mock- and HEXIM1-depleted NE (Fig. 2*B*, *lanes 3* and *4*), revealing a direct interaction between HEXIM2 and 7SK/P-TEFb independent of HEXIM1.

HEXIM1 and HEXIM2 Form Stable Homo- and Hetero-oligomers—Given the high degree of homology shared by HEXIM1 and HEXIM2 and their mutual interaction, it is possible that the individual HEXIM1 and HEXIM2 proteins may also form homo-oligomers. To test this possibility, cDNA constructs expressing FLAG- or HA-tagged HEXIM1 and HEXIM2 were co-transfected in different combinations into HeLa cells. Anti-FLAG immunoprecipitates derived from NE of the transfected cells were analyzed in parallel by anti-FLAG and anti-HA Western blotting. Indeed, HA-tagged HEXIM1 (Fig. 3*A*, *lane 2*) and HEXIM2 (*lane 7*) were found to co-immunoprecipitate with FLAG-tagged HEXIM1 and HEXIM2, respectively, demonstrating the abilities of both proteins to form homo-oligomers. In addition, formation of hetero-oligomers between HA-tagged HXM1 and FLAG-tagged HXM2 was also confirmed (*lane 4*). It is worth noting that the amount of the HEXIM homo-/hetero-oligomers was mostly unchanged by the RNase A-mediated removal of P-TEFb (data not shown) and 7SK from the immunoprecipitates (Fig. 3*A*, compare *lanes 2* and *3*, *4* and *5*, and *7* and *8*), indicating that these oligomers were stable and that their formations were most likely 7SK/P-TEFb-independent.

The HEXIM Homo-/Hetero-oligomers Can Be Detected as Part of the 7SK·P-TEFb snRNP—Although the different forms of HEXIM oligomers remained stable after the dissociation of 7SK and P-TEFb from the immunoprecipitates (Figs. 2*A* and 3*A*), it is not clear whether they existed in or outside the 7SK·P-TEFb snRNP. To resolve this issue, HeLa cells were co-transfected with the indicated combinations of FLAG- or HA-tagged HEXIM1 and HEXIM2 cDNA constructs (Fig. 3*B*). NE of the transfected cells was subjected to two successive rounds of immunoprecipitation, first with the anti-FLAG beads and then the anti-HA beads coupled with specific peptide elution after each precipitation. This procedure ensured that only homo- or hetero-oligomers containing both FLAG- and HA-tagged HEXIM1 and/or HEXIM2 would be obtained after the second round of immunoprecipitation; therefore, if any 7SK or P-TEFb were to be detected in the final precipitates, it must be associated with the HEXIM oligomers.

Indeed, CycT1 (data not shown), CDK9, and 7SK were all detected after the second round of purification from cells co-transfected with FLAG- and HA-tagged HEXIM1 (Fig. 3*B*, *lane 7*), FLAG- and HA-tagged HEXIM2 (*lane 9*), or FLAG-tagged HXM1 and HA-tagged HXM2 (*lane 8*). Control immunoprecipitations indicate that the detected signals were not due to any nonspecific binding of 7SK, P-TEFb, or FLAG-tagged HEXIM proteins to the anti-HA beads (*e.g.* compare *lane 5* with *lane 10* in Fig. 3*B*). Thus, the homo-/hetero-oligomers of HEXIM1 and HEXIM2 can be found within the 7SK·P-TEFb snRNP, although we cannot rule out the possible existence of a portion of the oligomers outside the snRNP (our glycerol gradient analysis in Fig. 7*B* suggests that this may well be the case).

For accuracy, the term "oligomers" has been used throughout this work to describe the HEXIM protein complexes. However, judging from the estimated size of the 7SK·HEXIM·P-TEFb snRNP in density gradient (see Fig. 7*B* and "Discussion"), it is highly likely that a HEXIM homo- or heterodimer exists as part of the 7SK snRNP. Because of its high stability and 7SK/P-TEFb-independent formation, the HEXIM dimers may function to nucleate the formation of the 7SK snRNP.

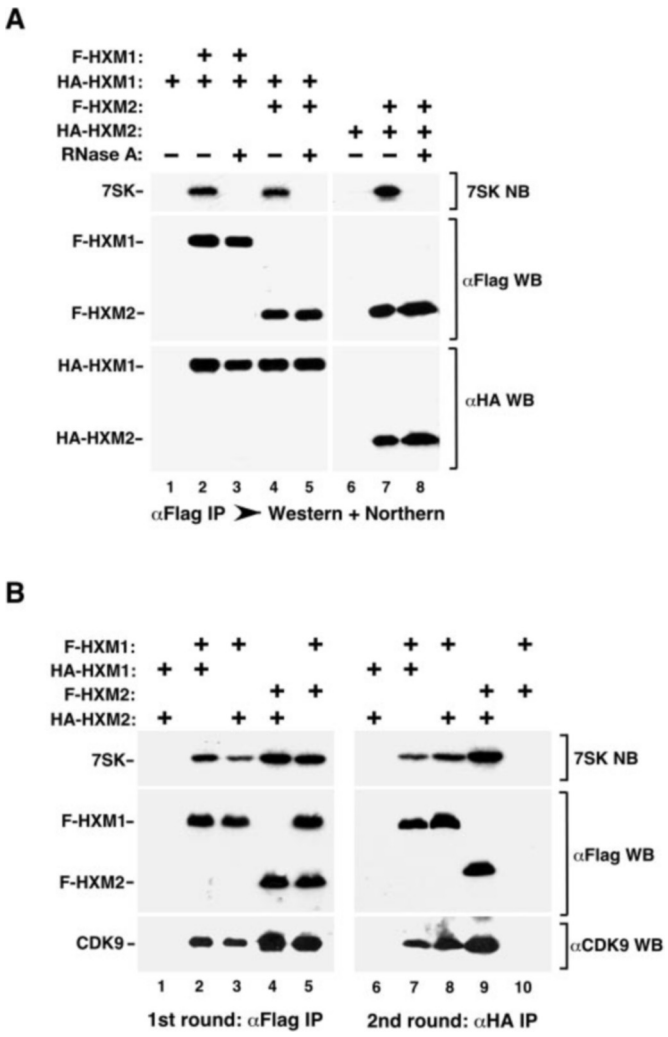

FIG. 3. **The HEXIM homo-/hetero-oligomers can be detected within the 7SK·P-TEFb snRNP.** *A*, HEXIM1 and HEIXM2 form homo-/hetero-oligomers. Various combinations of DNA constructs expressing FLAG- or HA-tagged HEXIM1 and HEXIM2 were co-transfected into HeLa cells as indicated. Anti-FLAG immunoprecipitates derived from NE of the transfected cells were analyzed by Northern blotting for 7SK RNA and Western blotting with anti-FLAG and anti-HA antibodies. *B*, HEXIM oligomers are detected inside the 7SK snRNP. NE prepared from cells transfected with the indicated combinations of FLAG-/HA-tagged HEXIM-expressing constructs were subjected to two rounds of immunoprecipitation, first with the anti-FLAG beads (*lanes 1–5*) and then with the anti-HA beads (*lanes 6–10*). The peptide-eluted samples after each round of precipitation were then analyzed by Northern and Western blotting as described in *A*.

HEXIM2-bound P-TEFb Is Transcriptionally Inactive—Combining the data above, we concluded that HEXIM2, as either a homo-oligomer or a hetero-oligomer with HEXIM1, was able to interact with core P-TEFb in a 7SK-dependent fashion. We next examined whether, like HEXIM1, HEXIM2 could also inhibit the transcriptional activity of P-TEFb. First, the core or 7SK/HEXIM2-bound P-TEFb complexes were affinity-purified (see "Experimental Procedures"), normalized for their CycT1 and CDK9 levels (Fig. 4, *left panel*), and tested for their abilities to restore transcription to the CDK9-depleted HeLa NE. As demonstrated previously (7, 19, 21), immunodepletion of CDK9 eliminated transcription (Fig. 4, *right panel*, *lane 1*). Addition of the core (Fig. 4, *right panel*, *lanes 4* and *5*), but not the 7SK/HEXIM2-bound P-TEFb (*lanes 2* and *3*), into the depleted NE restored promoter-distal transcription (elongation) from two G-less cassettes (G400 and G100) inserted, respectively, into two DNA

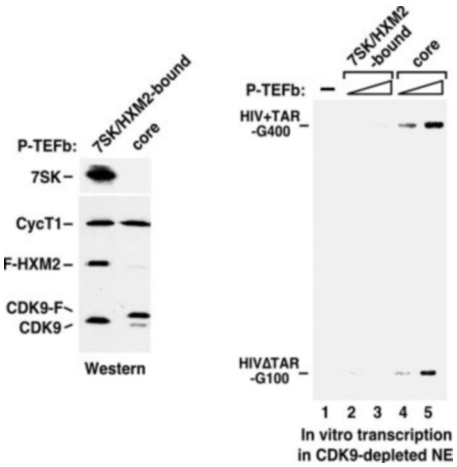

FIG. 4. **HEXIM2/7SK-bound P-TEFb is transcriptionally inactive.** The core and the HEXIM2/7SK-bound P-TEFb complexes were affinity-purified (see "Experimental Procedures"), normalized by Western and Northern blotting for their CycT1 and CDK9 levels (*left panel*), and then added to *in vitro* transcription reactions containing the CDK9-depleted HeLa NE and two transcription templates, HIV+TAR-G400 and HIVΔTAR-G100 (22), present in the same reaction (*right panel*). RNA fragments transcribed from two G-less cassettes inserted respectively into the two templates at a position ~1 kb downstream of the HIV-1 transcription start site are indicated.

templates (HIV+TAR-G400 and HIVΔTAR-G100) at ~1 kb downstream of the HIV-1 transcription start site (22). Thus, like HEXIM1 (7), HEXIM2 was also able to inhibit the transcriptional activity of the associated P-TEFb.

HEXIM2 Is Slightly More Effective than HEXIM1 in Inhibiting the Function of P-TEFb—We next compared the abilities of HEXIM1 and HEXIM2 to inhibit the kinase activity of P-TEFb. FLAG-tagged HEXIM1 and HEXIM2 proteins were affinity-purified from individually transfected cells under high salt plus RNase A conditions to remove the associated P-TEFb and 7SK (7, 11). Under these transient overexpression situations, no endogenous HEXIM2 was found to co-purify with F-HXM1 and vice versa (data not shown). Therefore, the interfering effect of the HEXIM1 and HEXIM2 hetero-oligomers is negligible. When similar amounts of F-HXM1 and F-HXM2 as confirmed by anti-FLAG Western blotting (Fig. 5*A*, *lanes 11* and *12*) were analyzed in kinase reactions, HEXIM2 (lanes 2 and 3) was found to be slightly more effective than HEXIM1 (*lanes 4* and *5*) in suppressing the ability of P-TEFb to phosphorylate GST-carboxyl-terminal domain. Furthermore, reflecting the 7SK-dependent HEXIM2·P-TEFb binding, inhibition of P-TEFb by HEXIM2 was also largely 7SK-dependent, as illustrated by the significantly reduced inhibition of P-TEFb activity when 7SK in the total HeLa nuclear RNA fraction was specifically cleaved by the 7SK antisense deoxyoligonucleotide-directed RNase H cleavage (Fig. 5*A*, compare *lanes 7* and *8* with *lanes 2* and *3*).

To investigate whether the inhibitory effects of HEXIM1 and HEXIM2 on the kinase activity of P-TEFb could lead to an inhibition of HIV-1 transcriptional elongation, we first examined the effects of HEXIM1 and HEXIM2 in an *in vitro* transcription assay containing normal HeLa NE. To help compare their relative activities, we chose the amounts of HEXIM proteins that would produce only a partial inhibition of transcription. When compared with the control reaction with no extra protein added (Fig. 5*B*, *lane 1*), exogenously added HEXIM2 (*lanes 4* and *5*) was slightly more efficient than HEXIM1 (*lanes 2* and *3*) in inhibiting RNA polymerase II elongation along the HIV-1 templates. Consistent with this result, transiently transfected HEXIM2 was also slightly more efficient in inhibiting the expression of a co-transfected luciferase reporter gene driven by the HIV-1 long terminal repeat (Fig. 5*C*). Taken together, the above data indicate that HEXIM2 was slightly more effective than HEXIM1 in inhibiting the kinase activity of P-TEFb to suppress transcription.

HEXIM1 and HEXIM2 Are Differentially Expressed in Various Human Tissues—Because HEXIM1 and HEXIM2 displayed similar abilities to suppress P-TEFb function, we next examined their mRNA expression patterns in various human tissues to gain insight into their tissue-specific functions. Northern analyses of 2 μg of total mRNA from an array of human tissues (Ambion) showed that the two forms of HEXIM1 mRNAs (~4 and 2.4 kb) described previously (23) were fairly ubiquitously expressed in all the tissues tested, except that there was a particularly high level of expression of the short form in the placenta (Fig. 6*A*, *lane 3*) and relatively low expression in the liver and pancreas. Compared with that of HEXIM1, the HEXIM2 mRNA (~1.5 kb) expression was more variable among different tissues, with relatively high expression detected in the brain (Fig. 6*A*, *lane 1*), liver (*lane 2*), colon (*lane 5*), and ovary (*lane 10*). In addition, there was a markedly increased expression of HEXIM2 of at least 20-fold in the testes (Fig. 6*A*, *lane 9*). In agreement with our observations, the data base present in SymAtlas (The Genomics Institute of the Novartis Research Foundation, symatlas.gnf.org/SymAtlas), which contains a compilation of gene expression profiles from 91 human and mouse samples across a diverse array of tissues, organs, and cell lines (24), also reported the highest expressions of HEXIM1 and HEXIM2 in placenta and testes, respectively. Thus, HEXIM1 and HEXIM2 are differentially expressed in various human tissues and may be utilized for different purposes specific to each tissue type.

Expressions of Both HEXIM1 and HEXIM2 Are Induced by HMBA—The expression of HEXIM1 in human vascular smooth muscle cells is induced by HMBA, a bipolar compound that has been shown to promote differentiation in cells of erythroid lineage (15). Because the effect of HMBA on the expression of the HEXIM protein family in other cell types has not been described extensively, we tested the effect of this compound on an array of human cell lines derived from different origins. Quantification of the Western data in Fig. 6*B* indicates that there was an overall induction of HEXIM1 protein expression in all the cell lines tested, with relatively mild (~2-fold) induction observed in HeLa, SK-Hep-1, and CaCo-2 cells and higher (~3–4-fold) induction observed in the rest. As for HEXIM2, HMBA treatment also slightly induced its expression by ~2-fold in U373, TK6, and CaCo-2 cells, whereas it remained undetectable in SK-Hep-1 and IMR-90 cells before and after the treatment. Notably, in 293T cells, HMBA treatment caused a significant increase in HEXIM2 expression from nearly undetectable to a very high level. Thus, although the induction of HEXIM1 and HEXIM2 by HMBA appears to be a general phenomenon in many cell types, the degree of induction varies among different cell lines.

HEXIM1 Is the Predominant Member of the HEXIM Family in HeLa and TK6 Cell Lines—To obtain accurate measurement of the relative levels of HEXIM1 and HEXIM2 in any given cell type, rabbit anti-HEXIM antibody that could recognize both HEXIM1 and HEXIM2 was generated against a conserved peptide shared by the two proteins (Fig. 1*A*). Based on quantification of the Western blot loaded with a serial dilution of cell lysates, HEXIM1 was found to be expressed at ~4-fold and ~6-fold higher than HEXIM2 in two established HeLa and TK6 cell lines, respectively.

Compensatory Contributions of HEXIM1 and HEXIM2 in Maintaining the Balance of Active and Inactive P-TEFb Complexes—Given the observation that HEXIM1 was ~4-fold more

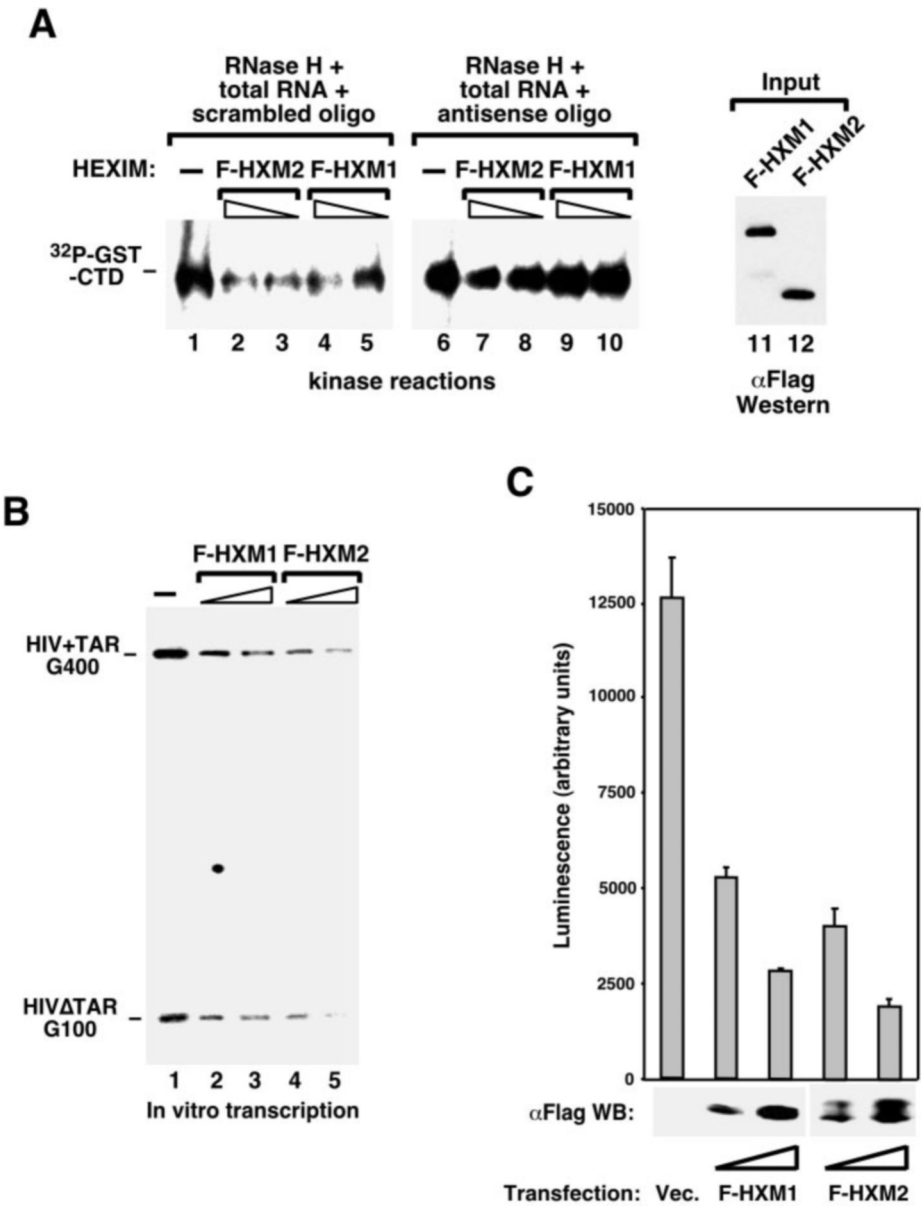

FIG. 5. **HEXIM2 is a slightly more efficient P-TEFb-inhibitor than HEXIM1.** *A*, inhibition of P-TEFb kinase activity by HEXIM1 and HEXIM2. *In vitro* kinase reactions containing P-TEFb as the kinase, GST-carboxyl-terminal domain as the substrate, and the HeLa total RNA fraction treated by RNase H cleavage in the presence of 7SK-antisense (*lanes 6–10*) or scrambled (*lanes 1–5*) deoxyoligonucleotide were performed. Similar amounts of FLAG-tagged HEXIM1 or HEXIM2 as determined by anti-FLAG Western blot (*lanes 11* and *12*) were added into the reactions to inhibit the P-TEFb kinase. Phosphorylated GST-carboxyl-terminal domain was detected by SDS-PAGE and autoradiography. *B*, inhibition of *in vitro* transcription by HEXIM1 and HEXIM2. Similar amounts of FLAG-tagged HEXIM1 or HEXIM2 were added into transcription reactions containing HeLa NE and a pair of HIV-1 transcription templates, HIV+TAR-G400 and HIVΔTAR-G100. RNA transcripts were analyzed as described in the Fig. 4 legend. *C*, inhibition of *in vivo* reporter gene expression by HEXIM1 and HEXIM2. HeLa cells were co-transfected with the HIV-1 long terminal repeat-luciferase reporter construct and the indicated plasmids for expressing HEXIM1 or HEXIM2 or only the empty vector. *Top panel*, luciferase activity was measured 48 h later, and data from three independent experiments are shown. *Bottom panel*, anti-FLAG Western analysis of the levels of the transfected FLAG-tagged proteins in whole cell lysate.

abundant than HEXIM2 in HeLa cells, we asked whether siRNA-mediated reduction in HEXIM1 gene expression would be compensated by an increase in the cellular level of HEXIM2. Data in the *left panel* of Fig. 7*A* indicate that whereas HEXIM1 expression was suppressed by the specific siRNA562 (7) to a level almost undetectable in HeLa NE, the nuclear levels of HEXIM2 as well as the other components of the 7SK·P-TEFb snRNP were not affected. Interestingly, although the level of HEXIM2 in NE remained unchanged by the HEXIM1-specific siRNA, more HEXIM2 could be found to associate with the anti-CDK9 immune complex derived from this NE as a result of the reduced HEXIM1 level (Fig. 7*A*, *right panel*).

To confirm this potential compensatory action of HEXIM2 in maintaining the balance of active and inactive P-TEFb complexes *in vivo*, glycerol gradient fractionation was used to examine the redistributions of the core and 7SK/HEXIM-bound P-TEFb complexes derived from HeLa cells expressing the HEXIM1-specific siRNA562 (Fig. 7*B*). Compared with molecular size standard analyzed in a parallel gradient as well as judging from the RNase A-mediated redistributions of CycT1, CDK9, and HEXIM in the gradient containing normal HeLa NE (Fig. 7*B*, compare the *top* and *middle panels*), it appeared that fractions 7 and 8 (a small portion also in fraction 6, ~300–400 kDa) contained the 7SK/HEXIM-bound P-TEFb, fractions 5 and 6 (mostly in fraction 5 and a small amount also in fraction 4) corresponded to the core P-TEFb, whereas frac-

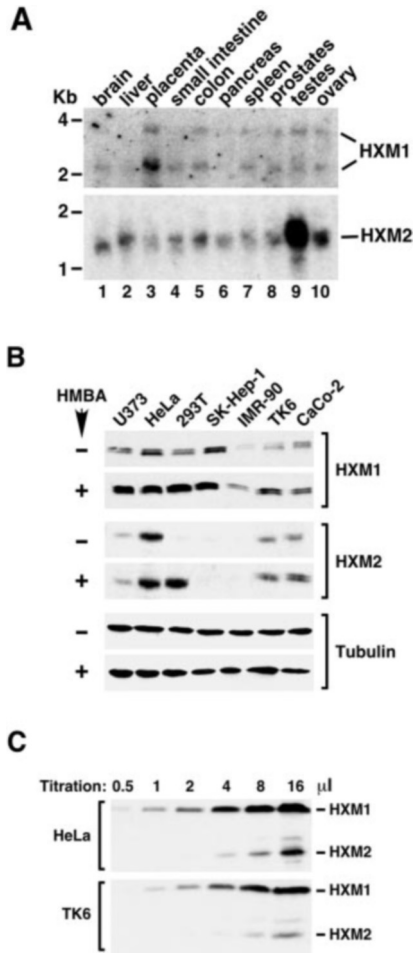

FIG. 6. **Differential expression of HEXIM1 and HEXIM2.** *A*, tissue distribution of HEXIM1 and HEXIM2 mRNAs. Two μg of poly(A)$^+$ RNAs from an array of indicated human tissues (FirstChoice^{TM} Northern Human Blot 2; Ambion) were hybridized to ^{32}P-labeled HEXIM1 or HEXIM2 antisense DNA probes. The HEXIM mRNAs were visualized by autoradiography. The same blot was used for both HEXIM1- and HEXIM2-specific probes with a stripping step performed in between. *B*, HMBA-induced expression of HEXIM1 and HEXIM2 in various human cell lines. The indicated cell lines grown to ~80% confluence were either treated with 10 mM HMBA for 22 h or left untreated. The levels of HEXIM1 and HEXIM2 in cell lysates were detected by Western blotting with the antibody that recognized both HEXIM proteins. Tubulin in the same lysates was used as a loading control. The tissue origins of the cell lines are as follows: U373, brain; HeLa, uterus; 293T, kidney; SK-HEP-1, liver; IMR-90, lung; TK6, spleen; and CaCo-2, colon. *C*, HEXIM2 is the minor member of the HEXIM family in HeLa and TK6 cells. Cell lysates were loaded in 2-fold increments on Western blot and detected with the antibody that recognized a conserved peptide shared by both HEXIM1 and HEXIM2. The HEXIM1 and HEXIM2 signals were then digitally quantified.

tions 2–4 represented mostly free monomeric subunits not associated with any complexes.

Whereas ~15% of the total HEXIM1 were co-sedimenting with P-TEFb in fractions 7 and 8 in normal HeLa NE, only a very small amount (~1.2%) of the total HEXIM2 was found associated with P-TEFb in these fractions (Fig. 7*B*, *middle panel*), indicating that HEXIM1 is the preferred binding partner for 7SK and P-TEFb under normal conditions. However, when the HEXIM1 level was reduced by siRNA562 (7), there was a significant redistribution of HEXIM2, resulting in ~18-fold more HEXIM2 associated with the 7SK·P-TEFb snRNP in fractions 7 and 8 (Fig. 7*B*, compare *middle* and *bottom panels*). Importantly, the distributions of the core and 7SK/HEXIM-bound P-TEFb complexes remained relatively unchanged in the presence or absence of HEXIM1 (compare CDK9 and CycT1 signals in Fig. 7*B*, *middle* and *bottom panels*). Taken together, the above co-immunoprecipitation and density gradient analyses strongly suggest that HEXIM2 can compensate for the loss of HEXIM1 in order to maintain a relatively stable level of the 7SK/HEXIM-bound P-TEFb *in vivo*.

DISCUSSION

In this study we show that the HEXIM1 homologue, HEXIM2, is a novel and integral component of the 7SK·P-TEFb snRNP, which plays an important role in sequestering P-TEFb into an inactive complex for suppression of transcriptional elongation. We have previously shown that the two regions most critical for HEXIM1 function are the arginine-rich 7SK-binding motif located within the central NLS and the P-TEFb-binding and inhibitory domain found in the carboxyl-terminal half (7, 11). Despite their distinct amino-terminal sequences, the NLS and carboxyl-terminal domains of HEXIM1 and HEXIM2 are >50% identical. This helps explain the similar abilities of HEXIM1 and HEXIM2 to inactivate the kinase and transcriptional activities of P-TEFb in a 7SK-dependent manner. It is perhaps also due to these functional similarities that HEXIM2 was able to compensate for the absence of HEXIM1 to maintain a constant amount of the 7SK/HEXIM-bound P-TEFb, suggesting an important requirement for cells to maintain a balance between active and inactive P-TEFb complexes.

Several lines of evidence have implicated that, as the primary binding partner and functional target of HEXIM1 (and presumably also HEXIM2), the general transcription factor P-TEFb plays an important role during the global control of cell growth and differentiation (7, 12, 16). For this reason, it is conceivable that the steady-state equilibrium between active and inactive P-TEFb complexes must be kept under strict cellular control. If this equilibrium is perturbed, as in the case of cardiac hypertrophy caused by hypertrophic signals (12) or possibly during breast cancer development caused by estrogens (16), serious physiological consequences can occur. Therefore, as demonstrated in this study, in the event of a sudden siRNA-mediated loss of HEXIM1 expression (thus creating the risk of producing excessive 7SK/HEXIM1-free, active P-TEFb), cells respond by mobilizing more HEXIM2 to bind to and maintain P-TEFb in the inactive state. This backup strategy attempts to restore the steady-state equilibrium of the active and inactive P-TEFb complexes in the absence of HEXIM1. However, probably due to the restricted tissue expression pattern of HEXIM2, which is largely non-overlapping with that of HEXIM1, or the unique amino-terminal domain of HEXIM2, which may confer an as yet unknown function different from that of HEXIM1, HEXIM2 apparently cannot completely replace HEXIM1 as the sole source of HEXIM proteins during embryonic development. This is illustrated by the observation that the ablation of the HEXIM1 (CLP-1) gene in mice leads to fetal death (13).

Combining several pieces of data presented here, it appears that HEXIM1 and HEXIM2 can form homo- as well as hetero-oligomers, both of which can be incorporated into the 7SK·P-TEFb snRNP. Assuming that only a dimer of HEXIM1 and/or HEXIM2 exists per 7SK snRNP (see discussion below), a minimum of three different types of 7SK snRNPs could potentially form. Although P-TEFb activity is similarly suppressed in all three snRNPs, it is not clear whether the three complexes serve completely identical or somewhat different functions under varying physiological conditions. Nevertheless, it is interesting to note that the interaction among the HEXIM proteins is independent of their associations with 7SK and P-TEFb. In fact, unlike the binding of 7SK and P-TEFb to the HEXIM proteins (7, 10), the HEXIM oligomers themselves are stable under high salt conditions (data not shown) and are not sub-

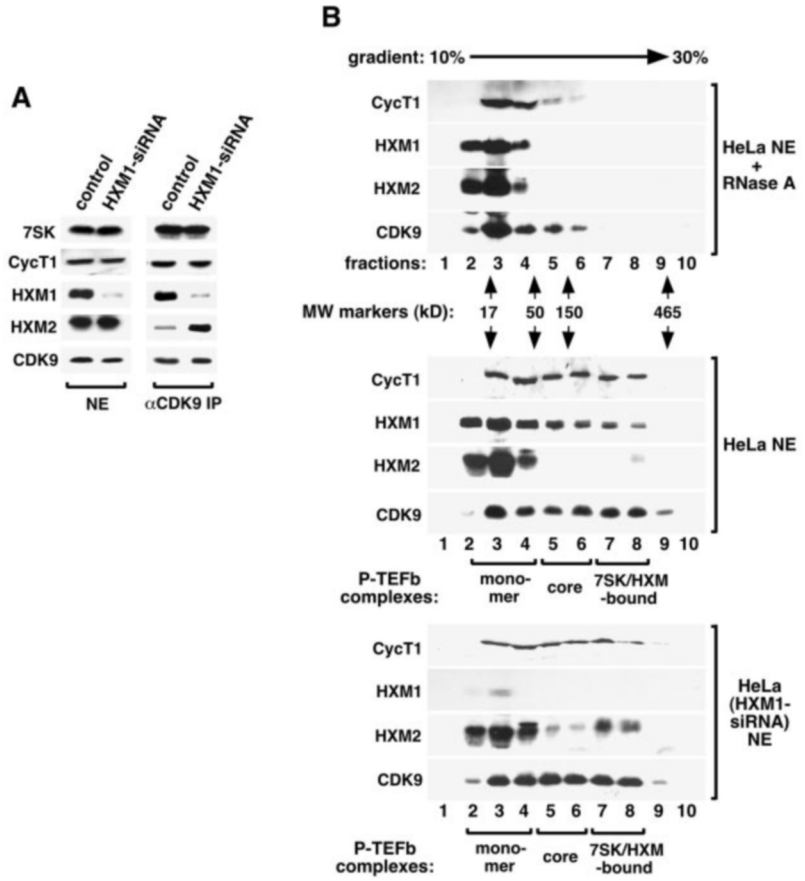

FIG. 7. **Compensatory action of HEXIM2 to maintain a constant level of 7SK snRNP *in vivo*.** *A*, siRNA-mediated reduction in HEXIM1 expression results in more HEXIM2 associated with the anti-CDK9 immunoprecipitates. The expression of HEXIM1 was suppressed by siRNA562 as described under "Experimental Procedures." The levels of individual 7SK snRNP components present in NE of control or the siRNA-expressing HeLa cells were analyzed by Western and Northern blotting in the *left panel*. The anti-CDK9 immunoprecipitates derived from the same extracts were analyzed in the *right panel*. *B*, HEXIM1-specific siRNA causes an increase in HEXIM2·P-TEFb binding as revealed by density gradient analysis. NE from HeLa cells expressing the HEXIM1-specific siRNA562 (*bottom panel*) was compared with standard HeLa NE treated with RNase A (*top panel*) or left untreated (*middle panel*) for distribution of CycT1, HEXIM1, HEXIM2, and CDK9 by glycerol gradient (10–30%) sedimentation. Gradient fractions were concentrated and analyzed by Western blotting. Molecular size standards were analyzed in a parallel gradient, and their positions in the gradient are indicated.

jected to dissociation caused by stress-inducing agents or degradation of the 7SK RNA scaffold (Fig. 3). Thus, the stable HEXIM oligomers may serve as the seed in nucleating the formation of the 7SK snRNP. At present, it is not known whether oligomerization of the HEXIM proteins is a prerequisite for their inhibitory action on P-TEFb. Future structural analyses of the complete 7SK·HEXIM·P-TEFb snRNP will provide insight into the role of the HEXIM oligomers in regulating the activity of P-TEFb.

The reported size of the native 7SK snRNP estimated by density gradient analysis is ~400–500 kDa (8). This size range is somewhat larger than our own estimation of ~300–400 kDa (Fig. 7*B*), which was obtained in standard Dignam HeLa NE (18). The size difference could be due to the fact that a different procedure was used in the previous report to prepare cell extracts for gradient analysis (8). Judging by the apparent size of each component, if the 7SK snRNP consists of a single copy of 7SK (~120 kDa), CDK9 (~40 kDa), and CycT1 (~85 kDa) and a homo-/heterodimer of the HEXIM proteins (2 × ~50–65 kDa), its size will be ~345–375 kDa. This calculation closely matches our observed size for the 7SK snRNP. On the other hand, if the intact 7SK snRNP contains two copies of each component (so far we have no evidence suggesting two copies of 7SK and P-TEFb present in the complex under normal conditions), the calculated size would reach ~590–620 kDa, which is considerably larger than the observed size range. We are keenly aware that this kind of size determination based on observed mobility of the complex in a density gradient is often unreliable, especially because the 7SK snRNP appeared to exist in a wider size range. It is perceivable that a range of complexes may exist and consist of HEXIM oligomers in different orders of multitude. More detailed structural studies of the 7SK snRNP, such as x-ray crystallography, are necessary to reveal the true composition of this complex in the cell.

The induction of HEXIM1 gene expression by the differentiation-inducing drug HMBA has been shown to be at the transcription level (14). Because the HEXIM2 locus is only 8.7 kb away from that of HEXIM1 on chromosome 17 (10), it is perhaps not too surprising to find that HEXIM2 can also be induced by HMBA, probably through a similar mechanism. Despite the close proximity between the HEXIM1 and HEXIM2 loci, the mRNA expression patterns of these two proteins are quite different in various human tissues. Whereas HEXIM1 is expressed rather uniformly in many tissues, HEXIM2 expression is more variable, with a particularly high level of HEXIM2 expression found in the testes (Fig. 6*A*). Future characterization of the promoter, 5′- and 3′-untranslated region sequences of these two genes may provide an answer to their tissue-specific expression patterns. We have noticed that the two forms of HEXIM1 mRNAs (~4 and 2.4 kb) generated due to alternate usage of poly(A) signals (23) are significantly longer than the HEXIM2 mRNA (~1.5 kb) and obviously contain quite extensive untranslated regions, which may be subjected to additional levels of gene expression control like those mediated by miRNA (25).

The HEXIM protein family apparently emerged late in evolution because homologues of both HEXIM1 and HEXIM2 are found only in mammals. With their similar P-TEFb-inhibitory function but different expression patterns, it is likely that the mammalian HEXIM1 and HEXIM2 genes evolved from a single ancestral HEXIM gene found in lower vertebrates. It is interesting to note that no HEXIM-related sequences are found in *Caenorhabditis elegans* or yeast (10). This is not surprising because the HEXIM-interacting partner 7SK is only conserved among vertebrates and is absent in worms or yeast (10). Thus, it appears that the HEXIM proteins, in conjunction with the 7SK snRNA, have co-evolved to provide a more advanced regulatory switch for fine-tuning the function of P-TEFb in verte-

brates. In addition, the emergence of two separate forms of HEXIM proteins with different tissue distribution patterns may provide a more versatile and complementary control of P-TEFb activity because highly complex organisms such as mammals are likely to require a more intricate mechanism for regulating transcriptional elongation during embryonic development, organ formation, and cellular differentiation.

Acknowledgments—We thank Dr. K. Luo for helpful suggestions and Vivien Lee for technical assistance.

REFERENCES

1. Sims, R. J., III, Belotserkovskaya, R., and Reinberg, D. (2004) *Genes Dev.* **18,** 2437–2468
2. Jones, K. A. (1997) *Genes Dev.* **11,** 2593–2599
3. Price, D. H. (2000) *Mol. Cell. Biol.* **20,** 2629–2634
4. Chao, S.-H., and Price, D. H. (2001) *J. Biol. Chem.* **276,** 31793–31799
5. Shim, E. Y., Walker, A. K., Shi, Y., and Blackwell, T. K. (2002) *Genes Dev.* **16,** 2135–2146
6. Yang, Z., Zhu, Q., Luo, K., and Zhou, Q. (2001) *Nature* **414,** 317–322
7. Yik, J. H., Chen, R., Nishimura, R., Jennings, J. L., Link, A. J., and Zhou, Q. (2003) *Mol. Cell* **12,** 971–982
8. Nguyen, V. T., Kiss, T., Michels, A. A., and Bensaude, O. (2001) *Nature* **414,** 322–325
9. Michels, A. A., Fraldi, A., Li, Q., Adamson, T. E., Bonnet, F., Nguyen, V. T., Sedore, S. C., Price, J. P., Price, D. H., Lania, L., and Bensaude, O. (2004) *EMBO J.* **23,** 2608–2619
10. Michels, A. A., Nguyen, V. T., Fraldi, A., Labas, V., Edwards, M., Bonnet, F., Lania, L., and Bensaude, O. (2003) *Mol. Cell. Biol.* **23,** 4859–4869
11. Yik, J. H., Chen, R., Pezda, A. C., Samford, C. S., and Zhou, Q. (2004) *Mol. Cell. Biol.* **24,** 5094–5105
12. Sano, M., Abdellatif, M., Oh, H., Xie, M., Bagella, L., Giordano, A., Michael, L. H., DeMayo, F. J., and Schneider, M. D. (2002) *Nat. Med.* **8,** 1310–1317
13. Huang, F., Wagner, M., and Siddiqui, M. A. (2004) *Mech. Dev.* **121,** 559–572
14. Ouchida, R., Kusuhara, M., Shimizu, N., Hisada, T., Makino, Y., Morimoto, C., Handa, H., Ohsuzu, F., and Tanaka, H. (2003) *Genes Cells* **8,** 95–107
15. Marks, P. A., Richon, V. M., Kiyokawa, H., and Rifkind, R. A. (1994) *Proc. Natl. Acad. Sci. U. S. A.* **91,** 10251–10254
16. Wittmann, B. M., Wang, N., and Montano, M. M. (2003) *Cancer Res.* **63,** 5151–5158
17. Morgenstern, J. P., and Land, H. (1990) *Nucleic Acids Res.* **18,** 3587–3596
18. Dignam, J. D., Lebovitz, R. M., and Roeder, R. G. (1983) *Nucleic Acids Res.* **11,** 1475–1489
19. Zhou, Q., Chen, D., Pierstorff, E., and Luo, K. (1998) *EMBO J.* **17,** 3681–3691
20. Chen, R., Yang, Z., and Zhou, Q. (2004) *J. Biol. Chem.* **279,** 4153–4160
21. Chen, D., Fong, Y., and Zhou, Q. (1999) *Proc. Natl. Acad. Sci. U. S. A.* **96,** 2728–2733
22. Zhou, Q., and Sharp, P. A. (1995) *EMBO J.* **14,** 321–328
23. Huang, F., Wagner, M., and Siddiqui, M. A. (2002) *Gene* (*Amst.*) **292,** 245–259
24. Su, A. I., Cooke, M. P., Ching, K. A., Hakak, Y., Walker, J. R., Wiltshire, T., Orth, A. P., Vega, R. G., Sapinoso, L. M., Moqrich, A., Patapoutian, A., Hampton, G. M., Schultz, P. G., and Hogenesch, J. B. (2002) *Proc. Natl. Acad. Sci. U. S. A.* **99,** 4465–4470
25. Bartel, D. P. (2004) *Cell* **116,** 281–297